The hypoxic response of tumors is dependent on their microenvironment

Barbara Blouw,[1] Hanqiu Song,[2] Tarik Tihan,[3] Jenel Bosze,[4] Napoleone Ferrara,[5] Hans-Peter Gerber,[5] Randall S. Johnson,[1] and Gabriele Bergers,[2,*]

[1]Molecular Biology Section, Division of Biological Sciences, University of California at San Diego, Pacific Hall Room 1212, MC-0366, 9500 Gilman Drive, La Jolla, California 92093
[2]Department of Neurosurgery and BTRC, University of California Comprehensive Cancer Center, University of California at San Francisco, HSE722, 513 Parnassus Avenue, San Francisco, California 94143
[3]Department of Pathology and BTRC, University of California at San Francisco, Neuropathology Unit HSW 408, 513 Parnassus Avenue, San Francisco, California 94143
[4]Neurobiology Section, Division of Biological Sciences, University of California at San Diego, 9500 Gilman Drive, La Jolla, California 92093
[5]Department of Molecular Oncology, Genentech Inc., South San Francisco, California 94080
*Correspondence: bergers@cgl.ucsf.edu

Summary

To reveal the functional significance of hypoxia and angiogenesis in astrocytoma progression, we created genetically engineered transformed astrocytes from murine primary astrocytes and deleted the hypoxia-responsive transcription factor HIF-1α or its target gene, the angiogenic factor VEGF. Growth of HIF-1α- and VEGF-deficient transformed astrocytes in the vessel-poor subcutaneous environment results in severe necrosis, reduced growth, and vessel density, whereas when the same cells are placed in the vascular-rich brain parenchyma, the growth of HIF-1α knockout, but not VEGF knockout tumors, is reversed: tumors deficient in HIF-1α grow faster, and penetrate the brain more rapidly and extensively. These results demonstrate that HIF-1α has differential roles in tumor progression, which are greatly dependent on the extant microenvironment of the tumor.

Introduction

Every tissue, including solid tumors, is dependent on adequate oxygen delivery. Angiogenesis, the formation of new blood vessels, is a discrete step in tumor progression that is required for the expansion of tumor mass (Folkman, 2000). The stage in which angiogenesis is initiated, however, can vary among tumors, depending on the type of malignancy and the microenvironment in which the tumor develops.

Astrocytomas, a class of malignant brain tumors, are very oxygen dependent (Brat et al., 2003). Interestingly, low-grade astrocytomas first acquire their blood supply by coopting existing normal brain blood vessels, without initiating angiogenesis. However, when grade III astrocytomas progress to grade IV astrocytomas/glioblastomas (the most malignant form of astrocytoma, also known as glioblastoma multiformae, or GBM), they show features of hypoxic and necrotic palisades. These palisades are in part caused by vessel regression (Holash et al.,

1999a) and increased tumor cell proliferation (Brat et al., 2002; Holland, 2000). The resultant hypoxia is then thought to induce new blood vessels that supply the tumor with the necessary metabolites (Brat et al., 2003). In fact, glioblastomas are in part defined by the appearance of proliferating endothelial cells and high blood vessel densities; these distinguish grade IV tumors from the lower grade astrocytomas histologically (Louis et al., 2001).

Hypoxic response is triggered to a large extent by the hypoxia inducible factor-1, or HIF-1, which is composed of a basic helix-loop-helix transcription factor dimer. This dimer has two components: HIF-1β, also known as ARNT, which is constitutively expressed, and HIF-1α, which is regulated posttranslationally by ubiquitination-triggered proteolysis (Semenza, 2002b). HIF-1 controls the expression of more than 40 target genes, whose protein products are implicated in angiogenesis, metabolism, and cell survival (Semenza, 2002a). Although three HIF-α proteins have been discovered, targeted deletion of the

SIGNIFICANCE

The role of hypoxia and angiogenesis in tumor progression has been modeled in numerous studies of malignancy in rodents; however, less well understood is the role that specific anatomic microenvironments play in determining hypoxic response and neovascularization in tumorigenesis. We show here that hypoxic response through the HIF-1α transcription factor plays dramatically different roles, depending on the tissue in which tumors are introduced. HIF-1α is a critical regulator of the production of angiogenic factors, including the vascular endothelial growth factor (VEGF); this study shows that target-directed therapies, including those that modulate hypoxic response, may have very different effects, dependent not on the cell type, or malignancy of the tumor, but on its location and microenvironment.

HIF-1α gene results in loss of hypoxic responsiveness of virtually every HIF-1-regulated transcript (Ryan et al., 2000).

Interestingly, HIF-1α is overexpressed in human glioblastoma biopsies, and the level of expression is correlated with highest grade of malignancy in human GBM (Zagzag et al., 2000). Among the most prominent target genes of HIF-1α is the angiogenic factor VEGF, which is also highly expressed in glioblastomas (Chaudhry et al., 2001). These data suggest that HIF-1α and VEGF may be tumor-promoting factors in astrocytoma progression.

Several laboratories have demonstrated that loss of the HIF-1α transcription factor results in reduced growth rates of various tumors, accompanied in some, but not all, models by decreased vascular density (Maxwell et al., 1997; Ryan et al., 1998, 2000). Other studies, however, have pointed in the opposite direction, describing HIF-1α as a tumor suppressor, whose loss gives rise to more aggressively growing embryonic stem cell-derived teratocarcinomas (Carmeliet et al., 1998). Thus, the role of the hypoxic response, and HIF-1α specifically, during tumor growth has been controversial.

One of the confounding variables in these studies has been the use of a range of cell types (e.g., hepatomas and fibrosarcomas) and different cell lines within those cell types (e.g., different embryonic stem [ES] cell lines). This makes comparative studies of the divergent tumors even more difficult to interpret, with respect to determining the actual role of hypoxic response during tumorigenesis in vivo.

One of the variables not extensively analyzed thus far in the experimental study of HIF-1α-deficient tumors is the relationship of site of malignancy to tumor progression. Most studies of tumor formation have been performed in immunocompromised mouse models at subcutaneous sites. Although this is a historic and well-studied site of tumor growth, the subcutaneous space has a number of intrinsic peculiarities that set it apart from sites elsewhere in the mammalian body. These include a lack of spatial constraints in the form of matrix or skeletal elements, relatively sparse vascularization, and the interface of a number of different tissue types (fat, muscle, connective tissue) found immediately under the skin.

The role of the tissue vasculature is particularly important when considering the hypoxic response of tumors. Tumors vary tremendously from tissue to tissue in degrees of invasiveness, levels of vascular density, and metastatic potential. How much of this variation is related to the state of the vasculature in the tissue itself? This is a particularly critical issue when studying the role of the HIF-1 transcription factor, which is activated by alterations in the microenvironment that are controlled by the local vasculature. It is important to note that many GBM studies still involve mouse models in which tumors grow subcutaneously, in a poorly vascularized environment (Huang et al., 1995; Ozawa et al., 1998; Prewett et al., 1999); this contrasts strongly with their natural habitat, the highly vascularized brain parenchyma.

We investigated whether HIF-1α activity and its downstream target, the angiogenic factor VEGF, are driving forces in astrocytoma progression by generating HIF-1α- and VEGF-deficient astrocytomas, and analyzed tumor propagation in two different microenvironments, the subcutaneous and intracranial habitat. Our study demonstrates that the HIF-1α-regulated hypoxic response to the microenvironment is highly dependent on the extant tissue microenvironment and involves VEGF-dependent and -independent mechanisms.

Results

Generation of HIF-1α-deficient (HIFko) astrocytomas

We isolated astrocytes from the hippocampus of mice homozygous for a HIF-1α/loxP allele (Figure 1A). To assure aggressive tumor formation, we immortalized and transformed them with SV40 large T antigen and the V12-H-ras oncogene, respectively (Figure 1A). V12H-ras was chosen because activation of the p21-ras pathway has been implicated in astrocytoma proliferation and angiogenesis (Feldkamp et al., 1999; Guha et al., 1997), and mouse strains expressing V12-H-ras under the control of a glial cell-specific promoter (GFAP) have been shown to develop high-grade astrocytomas (Ding et al., 2001). Similarly, SV40 large T antigen binds, and thereby inactivates, the two tumor suppressor proteins p53 and Rb that are commonly lost in astrocytoma progression (Louis et al., 2001; Xiao et al., 2002); in addition, transgenic mice expressing the Rb binding form of SV40 large T antigen in astrocytes also develop high-grade astrocytomas (Xiao et al., 2002).

To obtain HIF-1α-null (also known as HIFko) astrocytomas, we infected transformed HIF-1α loxP astrocytes with an adenovirus that expresses the bacteriophage recombinase Cre, or with a control virus expressing β-galactosidase. The recombinase efficiently deleted the floxed gene sequences present on the two conditional HIF-1α alleles, creating HIF-1α-deficient (HIFko) astrocytomas; real time-PCR analysis did not detect any nonrecombinant wild-type cells in adenoviral cre-infected cultures (data not shown). The adenovirus-treated control astrocytomas did not elicit any recombination and were defined as HIF-1α wild-type (also known as HIFwt) astrocytomas (Figure 1A). This multistep procedure allows a dissection of the role of HIF-1α in astrocytomas without the complications of using genetically altered and possibly diverged cell lines, because transformation is carried out prior to the removal of the HIF-1α gene by Cre recombinase activity; deletion then occurs at a very low passage number.

HIFko astrocytoma cells did not induce transcription of the HIF-1α-regulated genes phosphoglycerate kinase (PGK) and glucose transporter-1 (Glut-1) under hypoxic conditions, whereas HIFwt cells revealed 2- to 6-fold higher RNA levels of those genes when oxygen levels were decreased (Figure 1B). Slightly increased VEGF levels were still observed in HIFko cells because VEGF mRNA expression and stabilization is regulated by different mechanisms. Loss of hypoxic response through HIF-1α did not substantially affect cell growth of astrocytomas in vitro (Figure 1C), nor did it change the transformation status of those cells as evaluated in a soft agar assay (Figure 1D).

Subcutaneous growth of HIF-1α-deficient astrocytomas is impaired

We next assessed the role of HIF-1α transcriptional response in astrocytomas in a standard assay for tumorigenic potential in vivo, in which HIFwt and HIFko astrocytoma cell lines were injected subcutaneously into nude mice. Not only did HIFko astrocytomas grow more slowly than wild-type astrocytomas, reaching only 40% of the wild-type tumor weight at 21 days postinjection (Figure 2A), but there were also 30% fewer proliferating cells relative to wild-type astrocytomas (Figure 2B). Surprisingly, we did not observe any differences in the number of
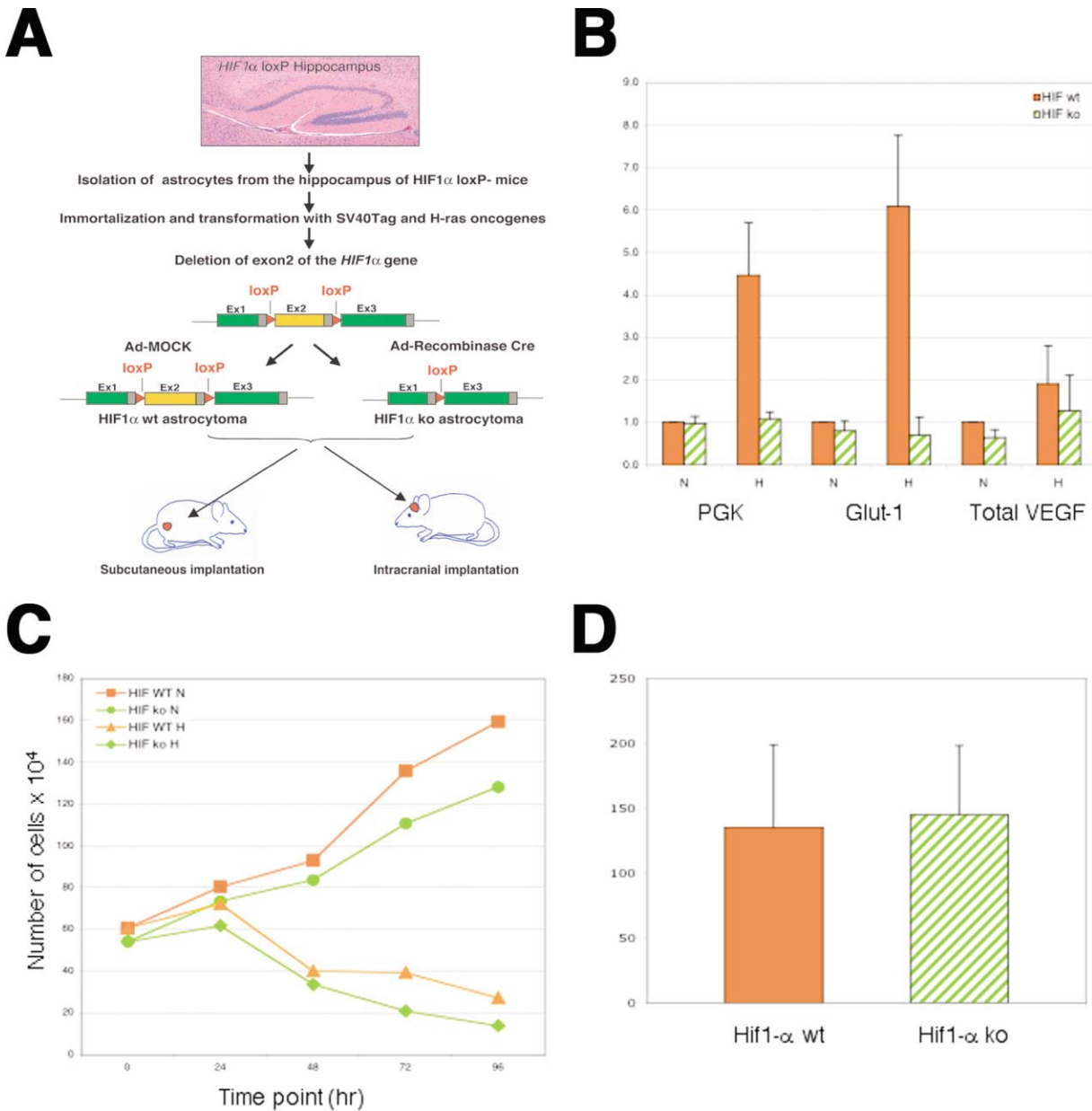
A

B

C

D

Figure 1. In vitro characterization of HIF-1α wild-type (HIFwt) and HIF-1α-deficient (HIFko) transformed astrocytes

A: Primary hippocampal astrocytes were isolated from HIF-1α loxP mice, immortalized, and transformed with SV40Tag and H-ras. HIF-1α-deficient transformed astrocytes were obtained with the bacteriophage recombinase Cre by deleting the floxed gene sequences of the HIF-1α alleles.

B: HIFwt and HIFko astrocytoma cells were cultured for 8 hr under hypoxic (0.5% pO$_2$) and normoxic (20% pO$_2$) conditions, harvested, and transcription levels of the hypoxia target genes *Pgk*, *Glut-1*, and *Vegf A* (all isoforms) determined by real-time PCR analysis. Induction of gene transcription was observed in HIFwt but not in HIFko astrocytes, under hypoxic conditions. Normoxia revealed similar expression levels of these genes in both cell lines. Error bars indicate SEM.

C: Growth rate of HIFwt and HIFko transformed astrocytes under normoxic (20% pO$_2$) and hypoxic (0.5% pO$_2$) conditions. The growth rates of HIF wt and HIFko cells did not differ under low and high oxygen conditions.

D: HIFwt and HIFko transformed astrocytes formed similar numbers and sizes of colonies in a soft agar colony formation assay. Error bars indicate standard deviation (SD).

apoptotic cells (Figure 2C). However, more than 70% of the small HIFko tumor nodules had hypoxic and necrotic areas, in contrast to wild-type control astrocytomas, which exhibited much smaller areas of hypoxic and necrotic palisades (Figures 2E and 2F). The morphology of the tumor cells in the two genotypes was indistinguishable (Figures 3A and 3B), and both wild-type and HIFko astrocytomas grew as encapsulated nodules (Figures 3C and 3D).

HIF-1α-deficient astrocytomas show increased cell proliferation in the brain but not in the subcutaneous habitat

We then injected HIFwt and HIFko astrocytomas intracranially into the brain parenchyma of nude mice, and compared the tumor phenotypes observed to the features of astrocytomas grown subcutaneously. Both HIFwt and HIFko astrocytomas showed typical features of high-grade gliomas: in particular,
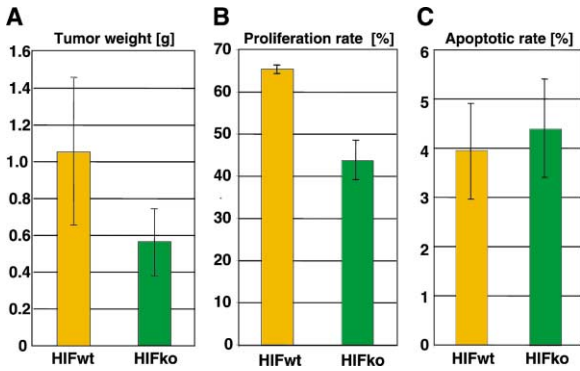
Figure 2. Growth comparison of HIFwt and HIFko astrocytoma in the subcutaneous space

A: Mice were inoculated subcutaneously with HIFwt and HIFko astrocytes, and tumors dissected after 21 days and weighed. HIFko astrocytomas had a reduced tumor weight of 60% compared to HIFwt tumors.

B: Proliferation index of HIFwt and HIFko tumors was assessed immunohistochemically by counting Ki-67 positive cells on tumor tissue sections. HIFko astrocytomas showed a 30% reduction in proliferation rate ($p < 0.0001$).

C: Apoptotic index of HIFwt and HIFko astrocytomas was quantified by TUNEL staining on tumor sections. There was no statistical difference in apoptotic cells between HIFwt and HIFko tumors ($p = 0.2345$). Error bars indicate standard deviation (SD).

they were fast growing, and elicited hypoxic and necrotic palisades. However, striking differences were observed. Mice bearing HIFwt or HIFko astrocytomas had similar survival times, of approximately 16–18 days (Figure 4C). This finding indicated that HIF-1α-deficient astrocytomas were not smaller than wild-type control tumors in the intracranial habitat which was confirmed by MRI (data not shown) and histopathological analyses (Figures 5A and 5B).

In contrast to subcutaneously grown astrocytomas, where the number of dividing cells declined by 30% in the absence of HIF-1α (Figure 2B), the number of proliferating cells in intracranial HIFko astrocytomas was 30% higher than that in wild-type tumors (Figure 4A). No differences in the apoptotic index were observed between wild-type and HIFko astrocytomas (Figure 4B).

Interestingly, HIFwt astrocytomas could often be distinguished morphologically from HIFko astrocytomas. Astrocytomas deficient in HIF-1α appeared more spindle-like than wild-type astrocytomas, which also contained mixed cell types (e.g., giant cells (Figures 5A and 5B). Most surprisingly, HIFko astrocytomas did not reveal large necrotic and hemorrhagic centers (Figures 5A–5D) but contained only small areas of hypoxic palisades, in contrast to the much larger areas seen in wild-type control astrocytomas (Figures 5C and 5D). It is important to note, however, that HIF-1α-deficient and wild-type astrocytomas were both defined as grade IV or mixed grade III/IV astrocytomas by our pathologist.

Loss of HIF-1α increases the invasive capacity of astrocytomas in the brain but not in the subcutaneous habitat

One important feature of both genotypes of astrocytomas was their diffuse growth into the brain parenchyma (Figures 5E–5H) that contrasted with the encapsulated phenotype of the same tumor lines grown subcutaneously (Figures 3C and 3D). The

infiltrative behavior of the intracerebrally placed tumors in fact nicely mimics the phenotypes observed in human astrocytomas. The tumor cells grew along existing blood vessels in the perivascular (Virchow-Robin) spaces in the brain (Figures 6C and 6D) and tracked along leptomeninges. To our surprise, however, HIFko astrocytomas invaded even into the collateral hemisphere, being detectable at different locations in both hemispheres of the brain (Figure 6B), as visualized by SV40 large T antigen staining (which specifically detects the injected tumor cells).

Although HIFwt astrocytomas were also diffusely growing (Figure 6C), they stayed focally localized—even at large sizes as illustrated in Figure 6A—whereas HIFko tumors did not. We were able to observe small clusters or even single HIF-1α-deficient tumor cells percolating throughout the brain parenchyma (Figure 6D), a feature of the diffusely growing tumor gliomatosis cerebrii. Covisualization of tumor cells and blood vessels revealed that HIFko astrocytomas had become extremely invasive, tracking along blood vessels in the perivascular space and moving along leptomeninges in both hemispheres (Figure 6D). In summary, loss of HIF-1α in tumors implanted in the brain had an almost diametrically opposed phenotype compared to the phenotype resulting from subcutaneous implantation. HIFko tumors had become more proliferative, and invasive, without showing features of large necrotic centers once implanted intracranially.

The microenvironment radically alters vascular structure and density in experimental astrocytomas, in a HIF-1α-dependent fashion

Based on the results above, we suspected that loss of HIF-1α might affect tumor vascularization differentially in these two tumor sites. We sought therefore to visualize and analyze the vascular phenotype of both subcutaneous and intracranial astrocytoma-derived tumors by perfusing the circulatory system with a fluorescent lectin (Figure 7). We found that subcutaneous HIFko astrocytomas were rather poorly vascularized, with small patches of distorted blood vessels that surrounded hypoxic and necrotic areas (Figure 7D), and vessel densities of only 52 vessels/mm^2 (Figure 7E). Wild-type astrocytomas contained 50% more blood vessels per unit area than subcutaneous HIFko tumors (105 vessels/mm^2; Figure 7E), a differential likely responsible in part for the relatively robust growth of the wild-type tumor cells at this site (Figures 7C and 7E).

Surprisingly, HIFko astrocytomas in the brain were not only highly vascularized (Figure 7B), but they also exhibited about 50% more blood vessels than the wild-type control astrocytomas (Figure 7E); this is the exact opposite of the finding in subcutaneous growth. The vessel density of HIFko tumors, however, was still lower than the vessel density of normal brain, a highly vascularized organ (380 vessels/mm^2 in normal brain versus 269 vessels/mm^2 in HIFko astrocytomas) (Figure 7E). It is important to note in this context that most tumors, including astrocytomas, exhibit a lower vessel density than the corresponding normal tissue because their oxygen consumption is lower than that of normal tissue (Eberhard et al., 2000; Hlatky et al., 2002). The majority of HIFko astrocytoma vessels resembled the morphology of the vascular network in normal brain (Figure 7B and 7F), appearing slim and organized. This is in contrast to blood vessels of HIFwt astrocytomas, which exhibited typical features of a tumor vasculature; i.e., the vessels were
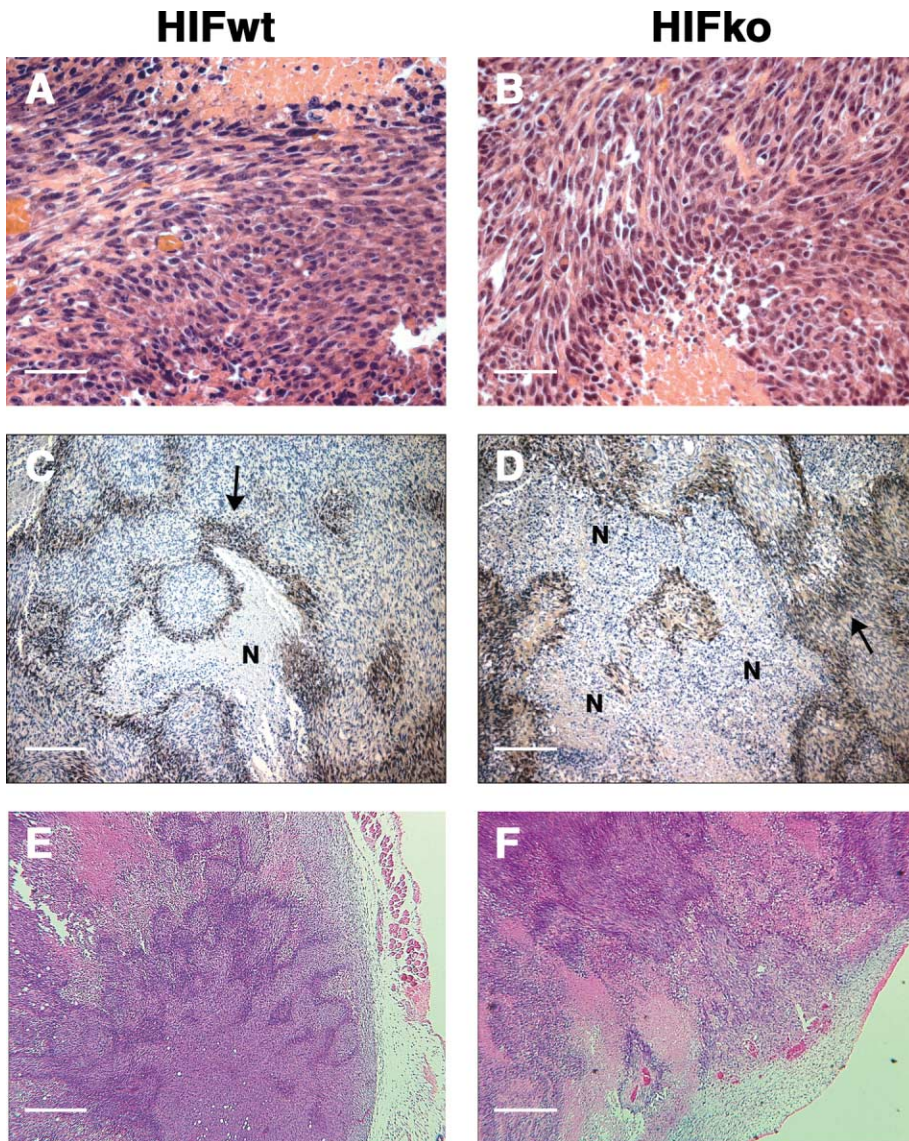
HIFwt

HIFko

Figure 3. Illustrative histopathology of subcutaneous HIFwt and HIFko astrocytomas

Hematoxylin & eosin (H&E) staining of HIFwt (**A**) and HIFko (**B**) astrocytomas (Bar = 40 μm). Tumor cells are morphologically similar. **C and D:** Hypoxia and necrosis in HIFwt and HIFko astrocytomas. Hypoxic areas (in brown) were visualized in tumors of pimonidazole-treated mice using the hypoxyprobe-1 monoclonal antibody (black arrow); necrotic areas are indicated as "N" (bar = 85 μm). HIFko astrocytomas are much more necrotic than HIFwt astrocytomas. **E and F:** Subcutaneous astrocytomas are encapsulated as visualized by H&E staining (bar = 200 μm).

irregularly shaped, distorted, dilated, and leaky, as indicated by extravasation of fluorescent lectin into the brain parenchyma (Figure 7A). The most striking differences in vascular morphology and density were apparent between HIFko astrocytomas in the subcutaneous area and brain. Subcutaneous tumors reduced to less than 20% in vessel density compared to intracranial HIFko tumors, only exposing small patches of distorted blood vessels (Figures 7E, 7B, and 7D) in contrast to the dense and elongated vasculature of HIFko tumors in the brain parenchyma. HIFwt astrocytomas had similar vessel densities in both settings, but with differences in vessel branching and morphology of the vasculature between the necrotic areas that covered the tumor (Figures 7A and 7C). The vasculature of subcutaneous HIFwt astrocytomas appeared less distorted, and showed signs of decreased branching, in comparison to the intracranial HIFwt astrocytomas (Figures 7A and 7C). The surprising result, that the vasculature of intracranial HIFko tumors resembles normal brain blood vessels, suggests that these tumors have not undergone neovascularization yet, but coopted the existing normal

brain vasculature. This would explain the increased degree of invasion of these fast-growing tumors, likely dictated by the necessity to retrieve sufficient oxygen and nutrients. If this hypothesis holds true, then one would expect differing levels of angiogenic factors in HIFwt and HIFko astrocytomas. What is the downstream factor of the HIF pathway that determines whether vessels will be coopted or neovascularization will be initiated?

Loss of VEGF limits tumor growth and regresses coopted blood vessels in the brain

VEGF-A (also known as VEGF) is highly expressed in grade IV astrocytomas/glioblastomas (GBM) and the most prominent angiogenic candidate, because its transcription is partly induced by the HIF-1 complex (Ferrara et al., 2003; Pugh and Ratcliffe, 2003). We analyzed VEGF RNA and protein levels in HIFwt and HIFko cell lines and tumors. VEGF RNA and protein was expressed in both cell lines under normoxic conditions, and was induced under hypoxic conditions, albeit to a lesser degree
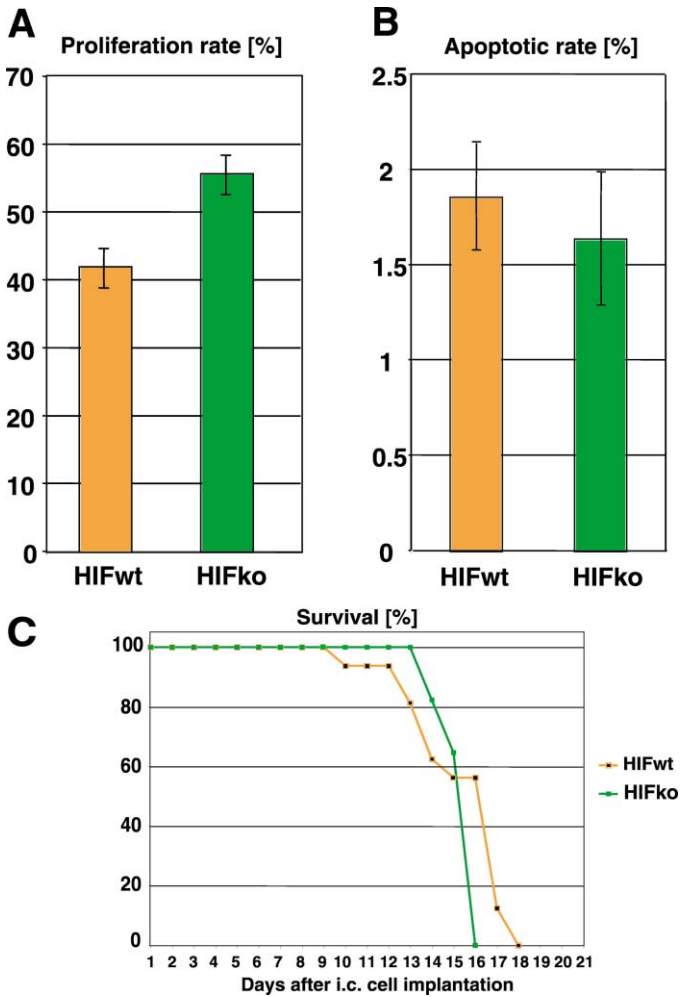
A Proliferation rate [%]

B Apoptotic rate [%]

C Survival [%]

Days after i.c. cell implantation

- HIFwt
- HIFko

Figure 4. Growth comparison of HIFwt and HIFko astrocytoma in the brain parenchyma

A: Mice were injected intracranially with HIFwt or HIFko astrocytoma and monitored daily. Mice were sacrificed as soon as they showed side effects of tumor expansion such as lateral recumbency and weight loss. Survival curves of mice bearing either HIFwt or HIFko astrocytomas are plotted. Mice had similar survival means (p = 0.129)

B: Proliferation index of HIFwt and HIFko tumors was assessed immunohistochemically by counting Ki-67 positive cells on tumor tissue sections. HIFko astrocytomas showed a 30% relative increase in the proliferation rate (p < 0.0001).

C: Apoptotic index of HIFwt and HIFko astrocytomas was quantified by TUNEL staining in tumor sections. There was no significant statistical difference in apoptotic cells between HIFwt and HIFko tumors (p = 0.1074). Error bars indicate standard deviation (SD).

HIFwt   **HIFko**

Figure 5. Illustrative histopathology of intracranial HIFwt and HIFko astrocytomas

H&E staining reveals hemorrhagic and necrotic areas (white arrow) and features of giant cells (black arrow) in HIFwt tumors (**A**), whereas HIFko tumors (**B**) often appear more spindle-like with little necrosis (bar = 45 μm). **C and D:** Detection of hypoxia and necrosis in HIFwt and HIFko astrocytomas. Hypoxic areas (in brown) were visualized in tumors of pimonidazole-treated mice using the hypoxyprobe-1 monoclonal antibody (black arrow); necrotic areas are indicated as "N." HIFko astrocytomas exhibit only small areas of hypoxia in contrast to HIFwt astrocytomas. H&E staining reveals a diffuse growth pattern of HIFwt (**E**) and HIFko astrocytomas (**F**) (bar = 95 μm) into the brain parenchyma that is confirmed by SV40 large T antigen staining (**G and H**) that detects injected tumor cells (bar = 95 μm).

in HIFko cells (Figures 1B and 7G). VEGF positive cells were also detected in intracranially and subcutaneously growing HIFwt and HIFko astrocytomas as revealed by immunohistochemical analysis (Supplemental Figures S1 and S2). Although the VEGF expression pattern was very heterogeneous at different areas within the tumors, intracranial HIFko tumors appeared to have overall lower levels of VEGF protein than the wild-type controls, whereas subcutaneous HIFwt and HIFko tumors both exhibited VEGF levels predominantly around perinecrotic palisades (Supplemental Figure S2).
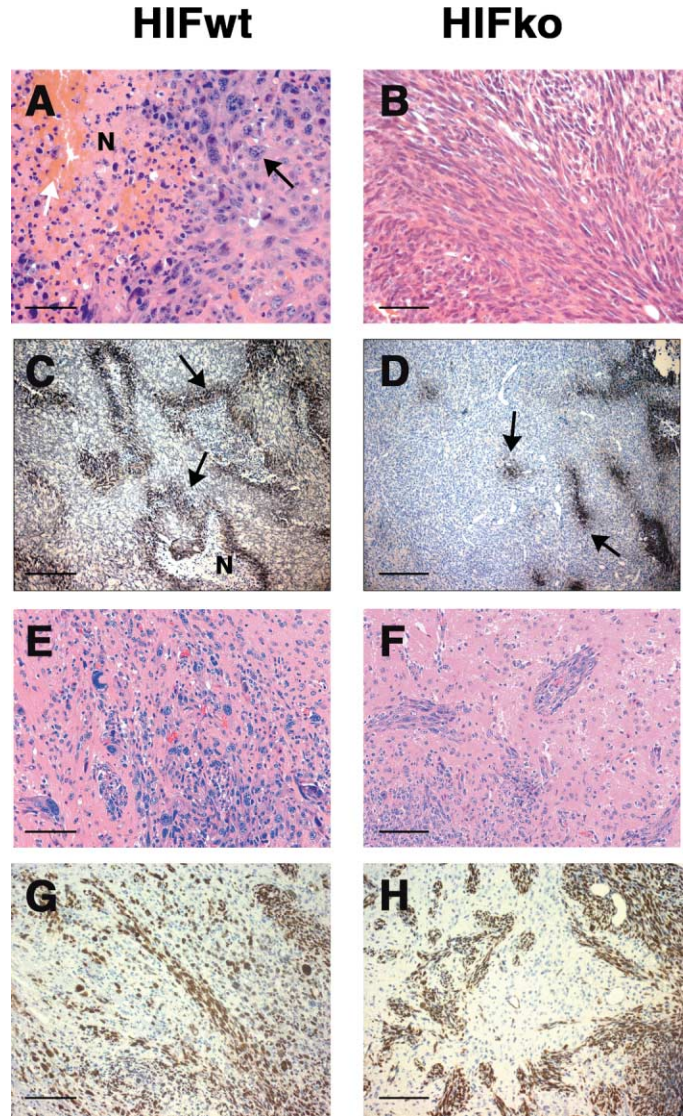
In order to determine whether the differing phenotypes ob-

served in HIFwt and HIFko astrocytomas are dependent on downstream activity of VEGF, we generated transformed astrocyte cell lines that were deficient in VEGF. Would tumors deficient in VEGF behave like those that are deficient in HIF-1α? We employed an approach similar to that described for the generation of HIFko astrocytomas (Figure 1A) by isolating astrocytes from VEGFloxP mice, wherein exon 3 of the *VEGF* gene is flanked by loxP recombination sites (Gerber et al., 1999).
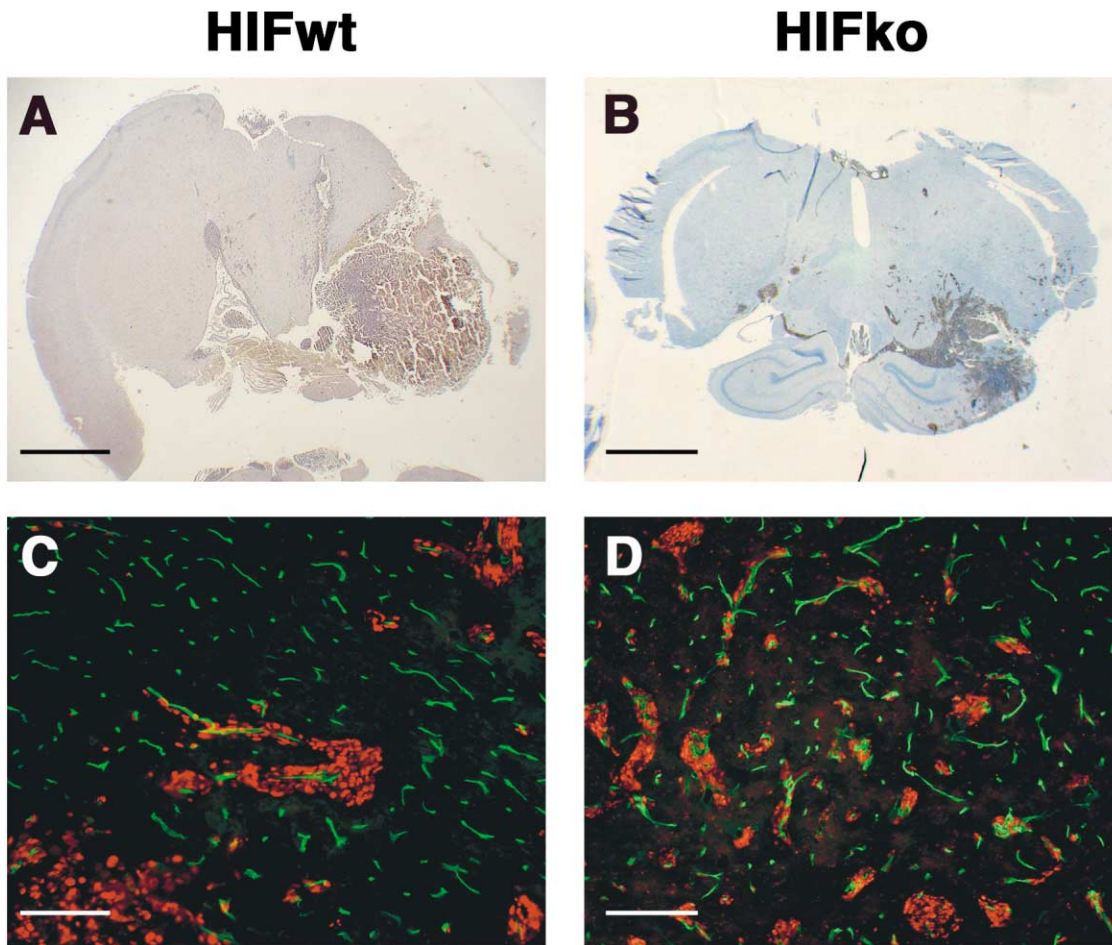
HIFwt

HIFko

Figure 6. Comparison of invasive behavior in intracranial HIFwt and HIFko astrocytomas

A and B: Invading tumor cells in the brain were detected by SV40 large T antigen staining (in brown). HIFko astrocytomas infiltrate both hemispheres of the brain (**B**; bar = 1.6 mm), whereas HIFwt astrocytomas, even at large sizes, (**A**, Bar = 1.3 mm) stay focally localized and expand at the site of implantation. **C and D:** Tumor-bearing mice were injected i.v. with FITC-labeled tomato lectin (lycopersicon esculentum) to stain blood vessels in green, and then heart-perfused with 4% paraformaldehyde (PFA), followed by immunohistochemical staining with Cy3-labeled SV40 large T antigen antibody to label tumor cells in red. Tumor cells are in close contact with normal brain blood vessels, and grow and migrate in the perivascular space. HIFko cells are detected in wide areas of the normal brain parenchyma (**C**), whereas HIFwt tumor cells are only detected around blood vessels close to the tumor mass (**D**).

We then immortalized and transformed VEGFloxP astrocytes with SV40Tag and V12H-ras oncogenes, and in situ excised the floxed exon 3 of the *VEGF* gene with an adenovirus expressing recombinase Cre (VEGFko astrocytomas). Infection with a control adenovirus expressing β-galactosidase was carried out as control, resulting in VEGF wild-type astrocytomas (also known as VEGFwt).

Both cell lines were then implanted subcutaneously and intracranially, tumor growth was observed, and dissected tumors were analyzed for their morphology, proliferation and apoptotic rates, and vascular profile. Similar to HIF-1α-deficient tumors, VEGFko astrocytomas grew much slower subcutaneously than the control VEGFwt tumors, reaching only about 50% of the wild-type tumor weight at 21 days postinjection (Figure 8A). We observed, however, striking differences between HIFko and VEGFko tumors in the brain. VEGFko astrocytomas grew slower than the control astrocytomas in the brain parenchyma, and mice had a statistically significant prolonged mean survival of 30%, compared to mice bearing VEGFwt tumors (p < 0.001)

(Figures 8B and 8C). VEGFko tumors in the subcutaneous habitat and brain elicited a significantly lower proliferation rate (Figure 8C), and exhibited a higher apoptotic rate than wild-type tumors (Figure 8D).

Histopathological analysis revealed more necrotic and hypoxic areas in subcutaneously growing VEGFko tumors compared to VEGFwt tumors (B.B., unpublished data) that can be partly explained by the 50% lower vascular density in VEGF-deficient subcutaneous astrocytomas (Figure 8E). These results are similar to those obtained from subcutaneous HIFko and HIFwt tumors (Figures 3A–3C and 7E). There were, however, significant differences between VEGFko and HIFko tumors in the brain parenchyma. VEGFko tumors (Figure 8Fb) did not form real tumor masses like VEGFwt (Figure 8Fa) or HIFko tumors (Figure 5B). Those tumors that were still defined as gradeIII/IV astrocytomas grew rather in migrating clusters, with necrosis in some of the centers that were encircled by vascular tumor nests (Figure 8Fb). Despite this diffusely growing phenotype, VEGF-deficient tumors were not detected in both brain hemi-
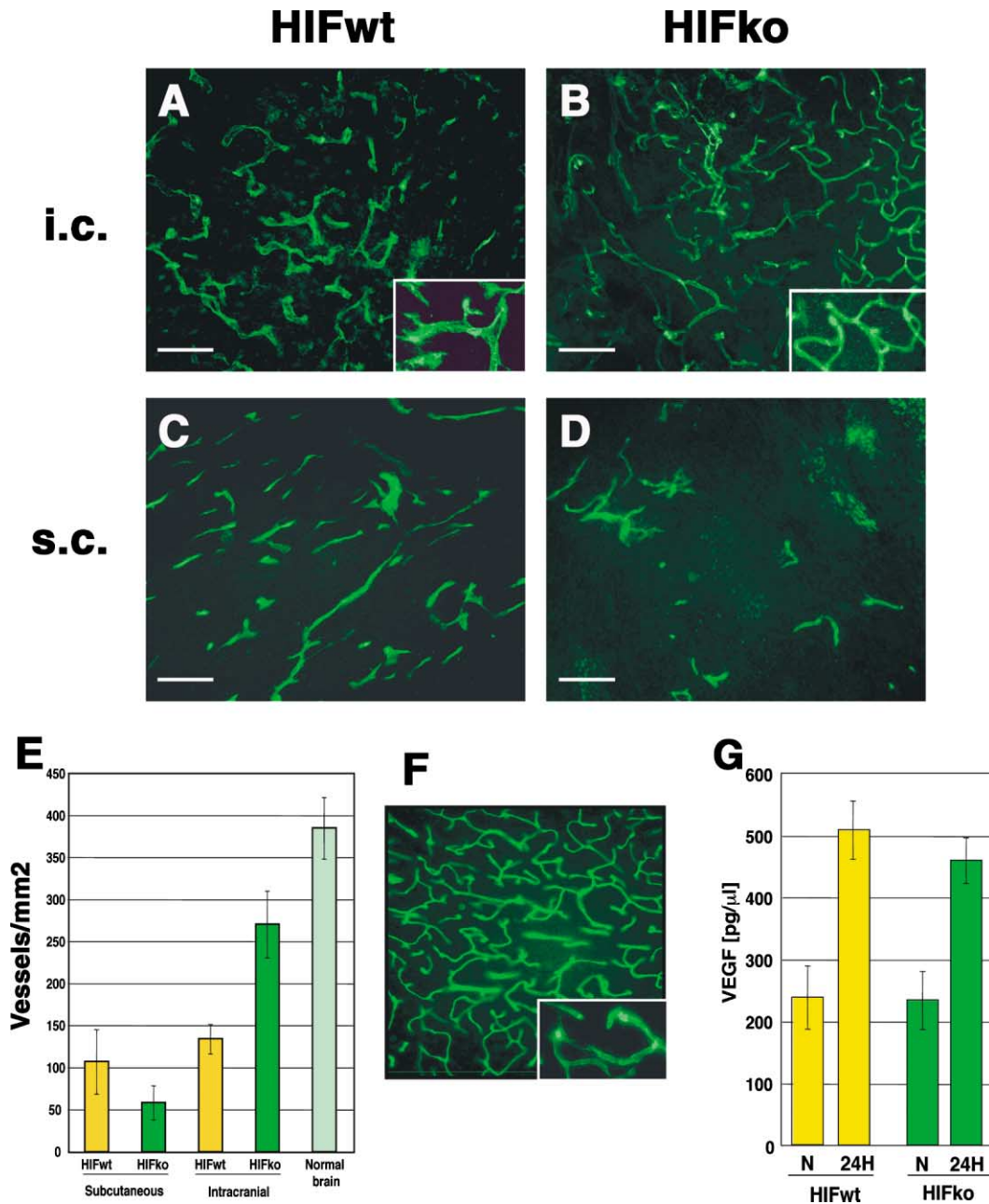
Figure 7. Comparison of vascular morphology and vessel density in HIFwt and HIFko astrocytomas grown in the subcutaneous and intracranial space

To visualize functional blood vessel, tumor-bearing mice were injected i.v. with FITC-labeled tomato lectin (lycopersicon esculentum) and then heart-perfused with 4% PFA. Brains were frozen in OCT medium and sectioned at 50 μm. The vasculature is visualized in green of intracranial (i.c.) HIFwt (**A**) and HIFko (**B**) astrocytomas, and subcutaneous (s.c.) HIFwt (**C**) and HIFko (**D**) astrocytomas (bar = 130 μm). **E:** Blood vessel density was assessed by counting vessels/mm^2 of 4–5 different tumors per group. Subcutaneous HIFko astrocytomas (**D** and **E**) show a 50% reduction in vessel density compared to s.c. HIFwt tumors (p = 0.0317) (**C** and **E**), exposing small patches of distorted and leaky vessels. In contrast, intracranial HIFko tumors are highly vascularized (5-fold higher than s.c. HIFko tumors) and reveal a 50% induction of vessel density in comparison to intracranial HIFwt astrocytomas (p = 0.0159) (**E**). Intracranial HIFko tumor vessels resemble normal brain blood vessels but show reduced vessel density in comparison to normal brain (**B** and **F**) in contrast to the distorted, dilated, and leaky vessels of intracranial HIFwt tumors in (**A**). **F:** Vasculature of normal brain. **G:** VEGF protein levels were assessed in conditioned medium of HIFwt and HIFko cells under normoxic and hypoxic (24 hr) conditions by an ELISA assay. VEGF protein levels are elevated in both cell lines under low oxygen levels.

spheres, but stayed focally localized, in striking contrast to the widespread dissemination of HIFko tumors. The distinct invasive patterns may be attributed to the differing vascular phenotype of both tumor types. Whereas HIFko tumors contained a dense network of more normal, elongated brain vessels (Figure 7B), VEGF-deficient tumors revealed a low density of distorted blood vessels; the vasculature was reduced by about 45% relative to VEGFwt tumors (Figures 8E, 8Fc, and 8Fd). The same relative
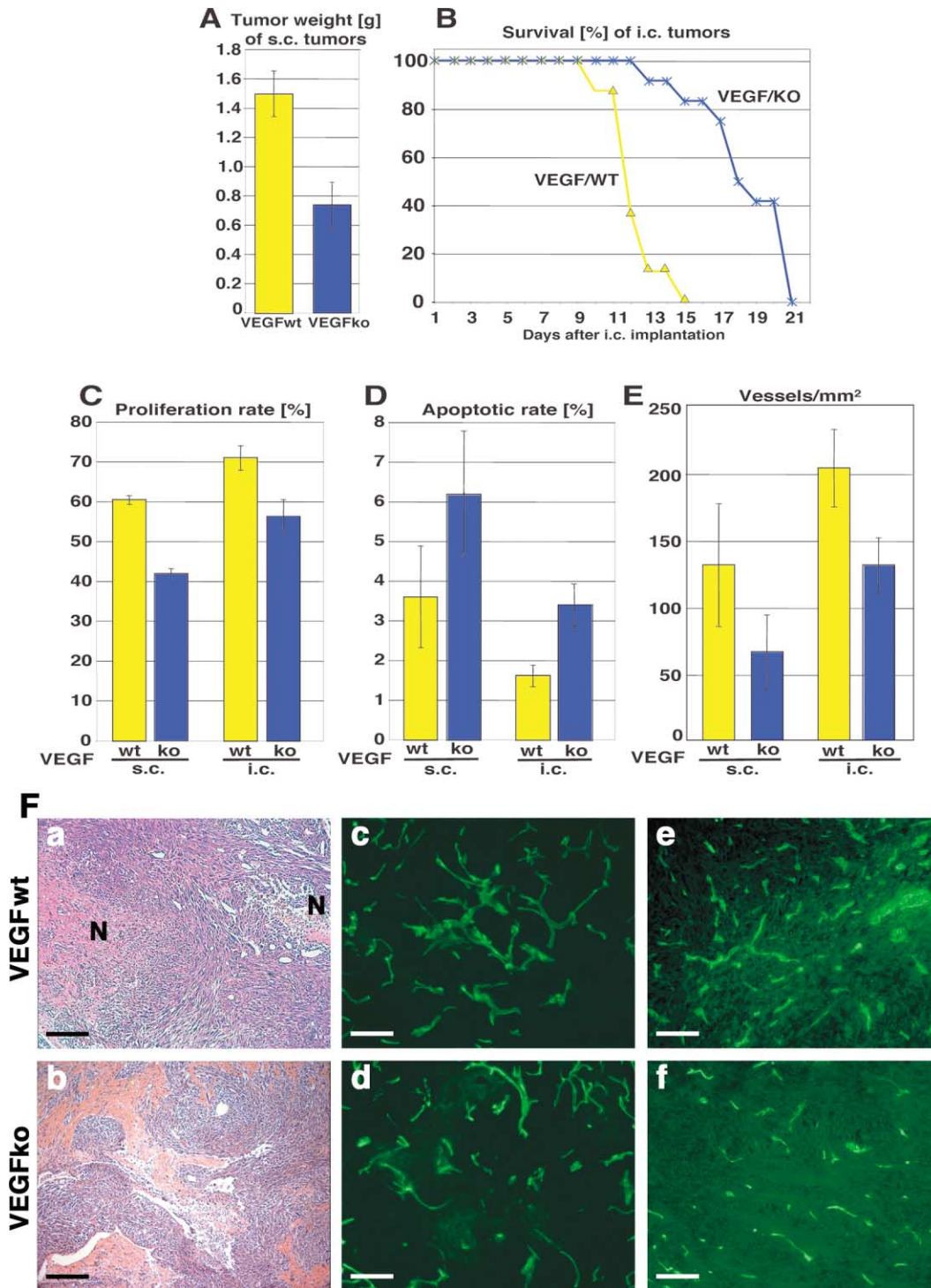
Figure 8. Comparison of cellular and vascular phenotypes of VEGFwt and VEGFko astrocytomas grown in subcutaneous (s.c.) and intracranial (i.c.) space

A: Mice were inoculated s.c. with VEGFwt and VEGFko astrocytomas, and tumors dissected after 21 days and weighed. The tumor weight of VEGFko astrocytomas was reduced by about 50% in comparison to VEGFwt tumors.

B: When mice were injected i.c. with VEGFwt and VEGFko tumors, mice bearing VEGFko tumors had a 35% longer survival mean than VEGFwt-tumor bearing mice (p < 0.001).

C and D: Proliferative (**C**) and apoptotic rate (**D**) of VEGFwt and VEGFko tumors was assessed immunohistochemically by counting Ki-67- or TUNEL-positive cells, respectively. The proliferation rate was significantly reduced in subcutaneously (p < 0.0001) and intracranially (p < 0.0001) grown VEGFko tumors. The apoptotic rate was increased in both s.c. (p = 0.0012) and i.c. (p = 0.0008) grown VEGFko tumors in comparison to VEGFwt tumors.

E: Blood vessel density was assessed by counting vessels/mm^2 of 4–5 fields of different tumors per group. Subcutaneous (p = 0.0303) and intracranial (p = 0.0159) VEGFko tumors showed a 40%–50% reduction in vessel density in comparison to the respective wt tumors. Error bars indicate standard deviation.

F: Illustrative histopathology and vascular morphology and density of VEGFwt and VEGFko astrocytomas. **a:** H&E staining reveals tumor masses of VEGFwt i.c. tumors with necrotic areas (N). **b:** VEGFko astrocytomas grow in migrating clusters without forming a real tumor mass. Blood vessels in i.c. (**c** and **d**) and s.c. (**e** and **f**) tumors are visualized with a FITC-labeled tomato lectin.

Table 1. Comparison of HIFko and VEGFko astrocytomas in the subcutaneous and intracranial environment

	HIFko versus HIFwt		VEGFko versus VEGFwt	
s.c.	Proliferation	↓	Proliferation	↓
	Apoptosis	○	Apoptosis	↑
	Vessel density	↓	Vessel density	↓
	Tumor growth	↓	Tumor growth	↓
	Invasion	no	Invasion	no
i.c.	Proliferation	↑	Proliferation	↓
	Apoptosis	○	Apoptosis	↑
	Vessel density	↑	Vessel density	↓
	Tumor growth	↑	Tumor growth	↓
	Invasion	↑↑	Invasion	↑

○, no change; ↑, induced; ↓, reduced.

vascular phenotype was observed in subcutaneously growing VEGFwt and VEGFko tumors; the vasculature of VEGFko tumors was also reduced by about 50% (Figures 8E, 8Fe, and 8Ff).

In summary, loss of VEGF in astrocytomas reduced subcutaneous and intracerebral tumor growth by severely impairing growth and survival of coopted tumor vessels. The tumors reacted differently to the regressing vessels: subcutaneous tumors became very necrotic, and showed increased apoptosis, whereas intracerebral tumors grew along blood vessels in migrating clusters, albeit only in close conjunction to the tumor (Table 1). Collectively, these results indicate that the hypoxic response of a tumor can determine initiation of new blood vessels, or cooption of existing blood vessels, but is highly dependent on the local environment in which those tumors arise.

Discussion

We have made the unexpected observation that HIF-1α can act as a negative or positive factor in astrocytoma progression, dependent on the microenvironment in which tumors grow. Loss of HIF-1α impairs astrocytoma growth subcutaneously, but increases proliferative and invasive properties of astrocytomas in the brain. These effects are not observed when VEGF, a downstream target of HIF-1α, is genetically ablated in astrocytomas (Table 1). VEGF-deficient astrocytomas exhibit a growth disadvantage in either microenvironment.

How can these opposite effects be explained? Hypoxia is a hallmark of grade IV astrocytomas/glioblastomas (GBM), and enables these tumors to partly induce angiogenesis in a HIF-1α-dependent manner. HIF-1α and its target VEGF are both highly upregulated in GBMs, and vascular proliferation is a prognostic marker in GBMs that distinguishes them from lower grade astrocytomas. In agreement with predicted behaviors of the tumors, our subcutaneous astrocytoma studies reveal that loss of HIF-1α, or VEGF, results in poorly vascularized tumors, and causes severe necrosis and restrained growth in the subcutaneous space. Thus, loss of HIF-1α or VEGF activity severely impaired astrocytoma growth. These data are in consensus with results of other laboratories: that absence of HIF-1α in ES cell-derived tumors resulted in reduced vascularization within the tumor due to a reduced capacity to induce VEGF expression by hypoxia (Carmeliet et al., 1998; Ryan et al., 1998; Tsuzuki et al., 2000). Similarly, genetic ablation of VEGF has been shown to cause a dramatic reduction in vascularity and growth of various tumors (Grunstein et al., 1999; Inoue et al., 2002; Tsuzuki et al., 2000).

The hypoxic response is dependent on the vascular microenvironment

What we did not expect was the radical change in tumor behavior when the site of implantation was changed from the commonly exploited subcutaneous site to a site much more reflective of the origin of these transformed cells, the intracranial space. In this microenvironment, HIF-1α-deficient tumors became more motile, moving along the perivascular spaces of normal blood vessels, and thereby infiltrating both hemispheres of the brain. Further, HIF-1α-deficient astrocytomas were better vascularized than the wild-type tumors, leading to a less necrotic phenotype in the brain. Nevertheless, the vessel density of HIFko tumors was lower than that of normal brain. It is important to note that it is a hallmark of most tumors that they exhibit a lower oxygen consumption rate, and therefore a lower vessel density, than the corresponding normal tissue, allowing tumor cells to accumulate between capillaries and thereby expanding the intercapillary distance (Eberhard et al., 2000; Hlatky et al., 2002). This also holds true for high-grade astrocytomas, because their microvessel density is lower than that of normal brain tissue (Eberhard et al., 2000).

Interestingly, low-grade astrocytomas first coopt existing brain vessels, and propagate along them; only when these tumors progress into grade IV astrocytomas/GBM do they become neovascularized. It is a peculiar feature of glioblastomas that they first regress the normal coopted blood vessels within the tumor mass before they form new tumor vessels; these are morphologically very distinct from the normal vasculature (Holash et al., 1999a, 1999b).

Blood vessel regression in astrocytomas is partly caused by Angiopoietin-2 (Ang2), a ligand of the receptor tyrosine kinase Tie-2, which is expressed in endothelial cells (Maisonpierre et al., 1997; Yancopoulos et al., 2000). Ang2 is induced early, when oxygen levels drop (Abdulmalek et al., 2001), and causes blood vessel regression in the absence of VEGF, but as soon as VEGF is induced, it will synergize with VEGF in new blood vessel formation (Hanahan, 1997). We have obtained preliminary data indicating that Ang2 levels are elevated in intracranial HIFwt, but not in HIFko astrocytomas (G.B. and Jocelyn Holash, Regeneron Inc., unpublished data). The high levels of Ang2 and the relatively low vessel density further support the notion that the vasculature of HIFwt tumors undergoes regression and remodeling as indicated by the appearance of more tortuous and distorted tumor blood vessels (Holash et al., 1999a, 1999b; Zagzag et al., 2000). In contrast, HIFko tumors express much lower levels of Ang 2 and consist of more densely packed elongated blood vessels, similar to vessels of normal brain, suggesting that these vessels have not undergone a transition to an angiogenic tumor vasculature.

Taken together, these observations suggest that HIF-1α-deficient astrocytomas are unable to induce angiogenesis, but that they adapt to this disadvantage by behaving like lower-grade astrocytomas; i.e., they take advantage of the highly vascularized environment, and migrate along existing normal blood vessels to propagate. Notably, HIFwt as well as HIFko astrocytomas were histopathologically both defined as grade III/IV or grade IV astrocytomas.

Based on these results, one would expect that VEGFko astrocytomas behave similarly to HIFko tumors, and exhibit increased invasive behavior in tumor cells, specifically around normal blood vessels in the brain parenchyma. Surprisingly,

VEGF-gene ablation in astrocytomas did not induce the phenotypes observed in HIFko astrocytomas when grown intracranially (summarized in Table 1). Whereas HIFko tumors grew faster than the wild-type tumors, VEGFko astrocytomas were at a growth disadvantage. This may be again attributed to their vascular phenotypes: in the brain, HIFko tumors were well vascularized, but VEGFko tumors were poorly vascularized. How can these discrepancies be explained? Loss of HIF-1α disables hypoxia-dependent VEGF induction, but we found that HIF-1α-deficient tumors still express VEGF, likely due to a combination of hypoxia-induced stabilization of VEGF mRNA, transcriptional induction by oncogenes such as H-ras, and VEGF expression of host cells within the tumor. The somewhat lower VEGF levels maybe sufficient to keep coopted brain vessels functional, but are not adequate to initiate angiogenesis. Moreover, other additional mechanisms, such as downregulation of angiogenic inhibitors like thrombospondin-1, might be necessary to induce the angiogenic switch (Watnick et al., 2003). The situation changes when VEGF is ablated in tumor cells: although tumors form nests around coopting blood vessels, those start to regress, which in turn keeps tumor cell proliferation limited. One may argue that the VEGF levels in intracranial VEGFko tumors, made by host cells, are not sufficient to support the existing vasculature of the growing tumor. The differing phenotypes of HIFko and VEGFko astrocytomas indicate that other factors than VEGF are likely to be involved in the adaptation of HIF-1α-deficient tumors to propagate without initiating angiogenesis. Importantly, the adaptation to become more invasive is also dependent on the microenvironment, suggesting an interaction between tumor cells and host factors in the extracellular matrix of the brain parenchyma.

Why do HIFko astrocytomas not coopt blood vessels in the subdermis, and become more invasive as they do in the brain? The subcutaneous environment is a very vessel-poor space that requires extensive recruitment and cooptation of vessels for tumor survival. In this context, loss of HIF-1α or VEGF, and subsequent loss of angiogenic capacity, is likely a negative factor, resulting in fewer vessels, less proliferation, and slower growth. This demonstrates that vessel recruitment and angiogenesis are parameters that affect tumor growth in highly variable ways. It is quite possible that the differing effects seen due to loss of HIF-1α in other laboratories are also tightly linked, not to the cell line involved, but to variations in the space in which transplanted tumors grow.

One could certainly argue that tumors deficient in HIF-1α may adapt other conduits to survive than the ones that we suggested above. Alternative paths by H-ras or p53-deficiency due to ectopic expression of SV40Tag can be likely excluded, because astrocytes were first transformed with these oncogenes before HIF-1α was deleted, leading to genetically identical cell lines, except for HIF-1α ablation. It is also unlikely that HIF-2α compensates for HIF-1α deficiency in the transformed astrocyte cells because we have analyzed HIF-2α protein levels in HIFwt and HIFko astrocytoma cell lines, and our preliminary data suggest that HIF-2α protein is present in our transformed astrocyte lines, but at low levels, and does not appear to be induced in the absence of HIF-1α (B.B., unpublished data).

Tumor-promoting effects of HIF-1α have been demonstrated by several groups (Maxwell et al., 1997; Ryan et al., 1998, 2000; Unruh et al., 2003). The role of HIF-1α as a potential "negative factor" in tumorigenesis has been implied by a smaller number of studies, although these have been exclusively embryonic stem cell-derived teratocarcinomas, injected subcutaneously (Carmeliet et al., 1998). Our study illustrates that the HIF-1α-mediated pathway can positively or negatively influence the fate and behavior of a tumor, such as an astrocytoma, but this influence is dependent upon the microenvironment. This is nicely demonstrated in the cell cycle regulation of HIFko astrocytomas. Loss of HIF-1α in astrocytomas in the brain revealed a higher proliferation index which is similar to the finding by Goda et al. that p53-deficient fibroblasts and B lymphocytes can be further pushed into cell cycle when HIF-1α is absent (Goda et al., 2003). The same transformed HIFko astrocytes, however, behave the opposite when transplanted into the subcutaneous space; i.e., they grow slower than the control astrocytomas, supporting the notion that the microenvironment is an additional crucial player in cell cycle regulation. Indeed, intracranial HIFko astrocytomas are not very hypoxic and necrotic and well vascularized, which is an environment that would favor tumor cell growth. In contrast, HIF-1α-deficient astrocytomas in the subcutaneous space are extremely hypoxic and necrotic and poorly vascularized, a harsh environment that limits tumor cell growth.

Implications for cancer therapy

Our observation of intracranial HIFko astrocytomas also has implications for therapy based on HIF-1α targeted inhibition. Our data suggest that inhibition of HIF-1α, thereby impairing the hypoxic response, might not be a desired strategy to treat astrocytomas, as they might adapt by becoming more invasive and infiltrative.

Interestingly, gene ablation of VEGF in astrocytomas exhibited a growth disadvantage both in the subcutaneous space and the brain, eliciting decreased proliferation rate and vessel density when compared to wild-type astrocytomas, arguing that regressing and impairing tumor vessels is a limiting step and a desired therapeutic approach for astrocytomas. This is in agreement with the findings that functional ablation of VEGF activity with a neutralizing antibody directed against VEGF resulted in vessel reduction, decreased tumor growth, and increased apoptosis in a rat model of glioblastomas (Rubenstein et al., 2000).

In summary, these results emphasize that the microenvironment has to be taken into consideration to better understand tumor behavior and adaptation in response to treatment modalities. Indeed, our findings are confirmed by several reports demonstrating that the microenvironment and tumor location functionally impacts tumor growth and metastasis. Many tumors have different behaviors when inoculated at sites different from their natural environment, most commonly in subcutaneous sites; they become encapsulated, lose their metastatic behavior, change their morphology, and, indeed, respond differently to treatment (Cuenca et al., 1996; MacDonald et al., 2001; Miyoshi et al., 2000; Taillandier et al., 2003).

Experimental procedures

Generation of *Hif1-α^WT* and *Hif1-α^{−/−}*, and *VEGFwt* and *VEGF^{−/−}*, transformed mouse astrocytes

Primary astrocytes were isolated from the hippocampus of 1- to 2-day-old HIF-1α+^{f}/+^{f} (HIFloxP) or VEGF+^{f}/+^{f} pups. HIF-1α+^{f}/+^{f} mice harbor flanked lox P sites of the second exon of the *Hif1-α* allele (Ryan et al., 2000), whereas VEGF+^{f}/+^{f} mice contain flanked lox P sites within exon 3 of the VEGF gene

(Gerber et al., 1999). Astrocytes of both mouse strains were isolated as follows: briefly, after removal of the meninges, the hippocampus was digested with papain (Worthington Biochemical Corporation, Lakewood, NJ) at a final concentration of 45 units/ml in a standard enzyme solution containing 50 mM EDTA, 150 mM $CaCl_2$, 100 mM L-cysteine, and 0.1 μg/ml Dnase in a solution consisting of 1 M HANKS, 10 mM HEPES (Invitrogen, Carlsbad, CA), and 7.5% $NaHCO_3$. The enzyme solution was aspirated and the digested tissue was washed in astrocyte tissue culture medium: BME supplemented with 10% FBS, 1% penicillin/streptomycin, 1% sodium pyruvate (all from Invitrogen), 0.6% glucose (Fisher, Los Angeles, CA), and 0.1% mito-serum extender (Becton Dickinson Biosciences, La Jolla, CA). Single-cell suspensions were cultured in the medium described and grown at 37°C in a humidified incubator containing 5% CO_2. After one week, primary astrocytes were purified by shaking the flasks on a rotator at RT at 300 rpm (Innova 2000, New Brunswick Scientific, Edison, NJ) and purity confirmed with an anti-GFAP antibody. Next, cells were immortalized by stable transfection with a SV-40 Large T antigen DNA construct. This was carried out by electroporation of pMC1neo Poly A (Stratagene, La Jolla, CA) and SV-40 Large T antigen using a BioRad Gene Pulser 2, set at 975 μF, ∞ resistance and 250 volts. Starting 48 hr posttransfection, stably transfected cells underwent G418 selection (300 μg/ml; Invitrogen). Resistant colonies were pooled and transformed by transfection of a retrovirus containing the H-Ras oncogene. Thereby, cells were plated in 6-well plates (Corning) at a density of 7×10^4 cells/well in BME and virus was added to the cells in combination with polybrene (Sigma, St. Louis, MO) at 4 μg/ml and medium. 48 hr postinfection, stably transfected cells were selected by Puromycin (Sigma) at a concentration of 1 μg/ml. After about 7 to 9 days, clones appeared, and they were pooled to obtain a heterogenous group of stably transformed cells, which were grown in the same medium, containing 5% FBS (Invitrogen). Next, the $Hif1$-α exon 2 was deleted by transfecting the cells transiently with an adenovirus expressing either cre recombinase or β-galactoside (MOCK). To determine the efficiency of $Hif1$-α deletion, genomic DNA was isolated from the cells and the recombination frequency was analyzed by TaqMan Real Time PCR analysis.

Growth curve and soft agar assay

For the growth curve, cells were plated in 12-well plates (Corning) in triplicates at a density of 1×10^5 cells/well in the described tissue culture medium for transformed astrocytes. Cells were exposed to normoxia 20% pO_2 and hypoxia 0.5% pO_2 for up to 96 hr. Cell counts were performed in duplicate at each time point using a hemacytometer. For the soft agar assay, cells were plated in triplicates in a 6-well plate at 5×10^5 cells/well, mixed in 0.35% LMP agarose (Invitrogen, Carlsbad, CA). After culturing the cells for 21 days, the wells were stained with 0.005% crystal violet for 4 hr and analyzed for colony number and size.

Real-time PCR assay

Cells were grown in 10 cm plates (Falcon) at 7×10^6 cells/plate and under normoxic and hypoxic conditions. After 8 hr incubation, total RNA was isolated using a Qiagen RNeasy kit according to the manufacturer's instructions. From 1 μg of total RNA, first-strand cDNA was synthesized using SUPERSCRIPT First-Strand (Invitrogen) according to the instructions of the manufacturer. For real-time PCR detection, 5 ng of input cDNA was analyzed in triplicate per primer pair per sample and the corresponding threshold cycle (Ct) values expressed as the mean $\pm$ s.e.m. All reactions were performed using 2$\times$ Taq Master Mix (Perkin Elmer Applied Biosystems), 900 nM of the forward and the reverse PCR primers, and 250 nM of a fluorescently tagged primer pair-specific probe in a total volume of 25 μl using default cycling parameters on an ABI Prism 7200 Sequence Detector. The following primer and probe sequences were used:

PGK-1: (F) 5′-CAGGACCATTCCAAACAATCTG-3′; (R) 5′-CTGTGGTAC TGAGAGCAGCAAGA-3′; (probe) 5′-(6FAM)TAGCTCGACCCACAGCCCTC GGCATAT-(TAMRA)-3′.

Glut-1: (F) 5′-ACGAGGAGCACCGTGAAGAT-3′; (R) 5′-GGGCATGTGC TTCCAGTATGT-3′; (probe) 5′-(6FAM) CAACTGTGCGGCCCCTACGTCTTC-(BHQ)-3′.

VEGF total: (F) 5′- ATCCGCATGATCTGCATGG-3′; (R) 5′-AGTCCCATG AAGTGATCAAGTTCA-3′; (probe) 5′- (6-FAM) TGCCCACGTCAGAGAGCAA CATCAC-(BHQ)-3′.

Subcutaneous implantation of *HIFwt* and *HIF*$^{-/-}$, and *VEGFwt* and *VEGF*$^{-/-}$ transformed astrocytes

22 athymic mice (4–6 weeks of age; Simonsen laboratory, San Jose, CA) were implanted subcutaneously with either 100 μl of 1×10^7 HIFwt, or 8 athymic mice with 1×10^7 VEGFwt transformed astrocytes. 21 athymic mice were injected subcutaneously with 100 μl of 1×10^7 HIFko or 8 mice with 1×10^7 VEGFko transformed astrocytes. 21 days postimplantation, tumors were harvested, weighed, and processed as described below for immunohistochemical analyses. All implantation experiments were repeated up to two times.

Intracranial implantation of HIFwt and HIF$^{-/-}$, and *VEGFwt* and *VEGF*$^{-/-}$ transformed astrocytes

35 athymic mice (4–6 weeks of age; Simonsen laboratory, San Jose, CA) were implanted intracranially with either 2.5 μl of 0.7×10^6 HIFwt or with 2.5 μl of 0.7×10^6 HIFko-transformed astrocytes. Similarly, six mice were injected with VEGFwt astrocytomas and eight mice with VEGFko-transformed astrocytes. Transplantation site was exactly 2 mm deep into the brain parenchyma and 3 mm to the right of the midline behind the breegma using a Hamilton syringe. All the mice were sacrificed between 15 to 21 days postimplantation when they showed side effects of tumor expansion such as lateral recumbency and weight loss. Mice were anesthetized, heart-perfused with 4% paraformaldehyde (PFA), and then brains either embedded into paraffin or frozen into OCT medium. All implantation experiments were repeated up to three times.

Visualization of the vasculature

To visualize blood vessels in tumors and normal tissue, mice were first anesthetized and injected (i.v.) with 0.05 mg FITC-labeled tomato lectin (*lycopersicon esculentum*; Vector Laboratories, Burlingame, CA) and then heart-perfused with 4% paraformaldehyde (PFA). Brains were frozen in OCT, sectioned at 50 μm, and appropriate sections mounted.

Detection of hypoxic areas in tumors

To allow assessment of the hypoxic regions within tumors, mice were injected i.p. with 60 mg/kg (in w/v PBS) pimonidazole (Hydroxyprobe-1TM, Natural Pharmacia International Inc.), 1.5 hr prior to sacrifice. Tumors were resected, processed, and embedded into paraffin. 5 μm sections were treated with 0.01% pronase for 40 min. at RT, washed, and incubated with Hydroxyprobe-1 mouse monoclonal antibody 1(MAb1; Natural Pharmacia International Inc) at a 1:50 dilution for 40 min at RT. A secondary biotinylated goat-anti mouse IgG antibody was applied, and staining visualized using the DAB chromophore (Vector ABC; DAB). Sections were rinsed and counterstained with hematoxylin.

Immunohistochemical analysis

HIFwt or HIFko astrocytoma cells in the brain were identified with a rabbit anti-SV40 Tag antibody. Briefly, slides were deparaffinized and incubated with the anti-Tag antibody (1:500; gift from Douglas Hanahan at UCSF) followed by treatment with a biotinylated goat anti-rabbit IgG antibody (1:200; Vector laboratories, Burlingame, CA). Antibody reactions were revealed with an ABC kit, using the chromophore 3,3-diaminobenzidine (DAB) substrate. For fluorescent detection, frozen tumor sections were stained with Tag antibodies and tumor cells visualized with a CY3-labeled goat anti rabbit IgG antibody (1:200; Jackson Immuno Research Laboratories, Inc).

In order to visualize tumor cells and the vasculature simultaneously, fluorescent immunohistochemistry was performed with the Tag antibody on brain cryosections of mice whose vascular system had been perfused FITC-Lectin prior to euthanasia.

Apoptotic index was assessed by TUNEL staining (Naik et al., 1996), and proliferating cells were detected with a rat anti-mouse Ki-67 antibody (1:100; DAKO Corporation, Carpinteria, CA) followed by incubation with a biotinylated rabbit-anti rat IgG antibody (1:200; Vector laboratories, Burlingame, CA) and DAB treatment as described above.

VEGF ELISA

HIFwt and HIFko transformed astrocyte cell lines were cultured under normoxia (20% pO_2) and incubated for 24 hr under hypoxic conditions (10% pCO_2; 0.5% pO_2). Conditioned medium was removed and VEGF levels were assayed by a sandwich DuoSet ELISA kit (DY493, R&D Systems, San Diego,

California), according to the manufacturer's instructions. Each assay condition was tested in triplicates.

Statistical analysis

References

Abdulmalek, K., Ashur, F., Ezer, N., Ye, F., Magder, S., and Hussain, S.N. (2001). Differential expression of Tie-2 receptors and angiopoietins in response to in vivo hypoxia in rats. Am. J. Physiol. Lung Cell. Mol. Physiol. *281*, L582–L590.

Brat, D.J., Castellano-Sanchez, A., Kaur, B., and Van Meir, E.G. (2002). Genetic and biologic progression in astrocytomas and their relation to angiogenic dysregulation. Adv. Anat. Pathol. *9*, 24–36.

Brat, D.J., Kaur, B., and Van Meir, E.G. (2003). Genetic modulation of hypoxia induced gene expression and angiogenesis: relevance to brain tumors. Front. Biosci. *8*, D100–D116.

Carmeliet, P., Dor, Y., Herbert, J.M., Fukumura, D., Brusselmans, K., Dewerchin, M., Neeman, M., Bono, F., Abramovitch, R., Maxwell, P., et al. (1998). Role of HIF-1α in hypoxia-mediated apoptosis, cell proliferation and tumour angiogenesis. Nature *394*, 485–490.

Chaudhry, I.H., O'Donovan, D.G., Brenchley, P.E., Reid, H., and Roberts, I.S. (2001). Vascular endothelial growth factor expression correlates with tumour grade and vascularity in gliomas. Histopathology *39*, 409–415.

Cuenca, R.E., Takita, H., and Bankert, R. (1996). Orthotopic engraftment of human lung tumours in SCID mice for the study of metastasis. Surg. Oncol. *5*, 85–91.

Ding, H., Roncari, L., Shannon, P., Wu, X., Lau, N., Karaskova, J., Gutmann, D.H., Squire, J.A., Nagy, A., and Guha, A. (2001). Astrocyte-specific expression of activated p21-ras results in malignant astrocytoma formation in a transgenic mouse model of human gliomas. Cancer Res. *61*, 3826–3836.

Eberhard, A., Kahlert, S., Goede, V., Hemmerlein, B., Plate, K.H., and Augustin, H.G. (2000). Heterogeneity of angiogenesis and blood vessel maturation in human tumors: implications for antiangiogenic tumor therapies. Cancer Res. *60*, 1388–1393.

Feldkamp, M.M., Lau, N., Rak, J., Kerbel, R.S., and Guha, A. (1999). Normoxic and hypoxic regulation of vascular endothelial growth factor (VEGF) by astrocytoma cells is mediated by Ras. Int. J. Cancer *81*, 118–124.

Ferrara, N., Gerber, H.P., and LeCouter, J. (2003). The biology of VEGF and its receptors. Nat. Med. *9*, 669–676.

Folkman, J. (2000). Tumor angiogenesis. In Cancer Medicine, Robert C. Bast, Jr., ed. (Hamilton, Ontario: BC Decker).

Gerber, H.P., Hillan, K.J., Ryan, A.M., Kowalski, J., Keller, G.A., Rangell, L., Wright, B.D., Radtke, F., Aguet, M., and Ferrara, N. (1999). VEGF is required for growth and survival in neonatal mice. Development *126*, 1149–1159.

Goda, N., Ryan, H.E., Khadivi, B., McNulty, W., Rickert, R.C., and Johnson, R.S. (2003). Hypoxia-inducible factor 1α is essential for cell cycle arrest during hypoxia. Mol. Cell. Biol. *23*, 359–369.

Grunstein, J., Roberts, W.G., Mathieu-Costello, O., Hanahan, D., and Johnson, R.S. (1999). Tumor-derived expression of vascular endothelial growth factor is a critical factor in tumor expansion and vascular function. Cancer Res. *59*, 1592–1598.

Guha, A., Feldkamp, M.M., Lau, N., Boss, G., and Pawson, A. (1997). Proliferation of human malignant astrocytomas is dependent on Ras activation. Oncogene *15*, 2755–2765.

Hanahan, D. (1997). Signaling vascular morphogenesis and maintenance. Science *277*, 48–50.

Hlatky, L., Hahnfeldt, P., and Folkman, J. (2002). Clinical application of antiangiogenic therapy: microvessel density, what it does and doesn't tell us. J. Natl. Cancer Inst. *94*, 883–893.

Holash, J., Maisonpierre, P.C., Compton, D., Boland, P., Alexander, C.R., Zagzag, D., Yancopoulos, G.D., and Wiegand, S.J. (1999a). Vessel cooption, regression, and growth in tumors mediated by angiopoietins and VEGF. Science *284*, 1994–1998.

Holash, J., Wiegand, S.J., and Yancopoulos, G.D. (1999b). New model of tumor angiogenesis: dynamic balance between vessel regression and growth mediated by angiopoietins and VEGF. Oncogene *18*, 5356–5362.

Holland, E.C. (2000). Glioblastoma multiforme: the terminator. Proc. Natl. Acad. Sci. USA *97*, 6242–6244.

Huang, P., Allam, A., Taghian, A., Freeman, J., Duffy, M., and Suit, H.D. (1995). Growth and metastatic behavior of five human glioblastomas compared with nine other histological types of human tumor xenografts in SCID mice. J. Neurosurg. *83*, 308–315.

Inoue, M., Hager, J.H., Ferrara, N., Gerber, H.P., and Hanahan, D. (2002). VEGF-A has a critical, nonredundant role in angiogenic switching and pancreatic beta cell carcinogenesis. Cancer Cell *1*, 193–202.

Louis, D.N., Holland, E.C., and Cairncross, J.G. (2001). Glioma classification: a molecular reappraisal. Am. J. Pathol. *159*, 779–786.

MacDonald, T.J., Taga, T., Shimada, H., Tabrizi, P., Zlokovic, B.V., Cheresh, D.A., and Laug, W.E. (2001). Preferential susceptibility of brain tumors to the antiangiogenic effects of an alpha(v) integrin antagonist. Neurosurgery *48*, 151–157.

Maisonpierre, P.C., Suri, C., Jones, P.F., Bartunkova, S., Wiegand, S.J., Radziejewski, C., Compton, D., McClain, J., Aldrich, T.H., Papadopoulos, N., et al. (1997). Angiopoietin-2, a natural antagonist for Tie2 that disrupts in vivo angiogenesis. Science *277*, 55–60.

Maxwell, P.H., Dachs, G.U., Gleadle, J.M., Nicholls, L.G., Harris, A.L., Stratford, I.J., Hankinson, O., Pugh, C.W., and Ratcliffe, P.J. (1997). Hypoxia-inducible factor-1 modulates gene expression in solid tumors and influences both angiogenesis and tumor growth. Proc. Natl. Acad. Sci. USA *94*, 8104–8109.

Miyoshi, T., Kondo, K., Ishikura, H., Kinoshita, H., Matsumori, Y., and Monden, Y. (2000). SCID mouse lymphogenous metastatic model of human lung cancer constructed using orthotopic inoculation of cancer cells. Anticancer Res. *20*, 161–163.

Naik, P., Karrim, J., and Hanahan, D. (1996). The rise and fall of apoptosis during multistage tumorigenesis: down-modulation contributes to progression from angiogenic progenitors. Genes Dev. *10*, 2105–2116.

Ozawa, T., Wang, J., Hu, L.J., Lamborn, K.R., Bollen, A.W., and Deen, D.F. (1998). Characterization of human glioblastoma xenograft growth in athymic mice. In Vivo *12*, 369–374.

Prewett, M., Huber, J., Li, Y., Santiago, A., O'Connor, W., King, K., Overholser, J., Hooper, A., Pytowski, B., Witte, L., et al. (1999). Antivascular endothelial growth factor receptor (fetal liver kinase 1) monoclonal antibody

inhibits tumor angiogenesis and growth of several mouse and human tumors. Cancer Res. *59*, 5209–5218.

Pugh, C.W., and Ratcliffe, P.J. (2003). Regulation of angiogenesis by hypoxia: role of the HIF system. Nat. Med. *9*, 677–684.

Rubenstein, J.L., Kim, J., Ozawa, T., Zhang, M., Westphal, M., Deen, D.F., and Shuman, M.A. (2000). Anti-VEGF antibody treatment of glioblastoma prolongs survival but results in increased vascular cooption. Neoplasia *2*, 306–314.

Ryan, H.E., Lo, J., and Johnson, R.S. (1998). HIF-1α is required for solid tumor formation and embryonic vascularization. EMBO J. *17*, 3005–3015.

Ryan, H.E., Poloni, M., McNulty, W., Elson, D., Gassmann, M., Arbeit, J.M., and Johnson, R.S. (2000). Hypoxia-inducible factor-1α is a positive factor in solid tumor growth. Cancer Res. *60*, 4010–4015.

Semenza, G.L. (2002a). HIF-1 and tumor progression: pathophysiology and therapeutics. Trends Mol. Med. *8*, S62–S67.

Semenza, G.L. (2002b). Involvement of hypoxia-inducible factor 1 in human cancer. Intern. Med. *41*, 79–83.

Taillandier, L., Antunes, L., and Angioi-Duprez, K.S. (2003). Models for neuro-oncological preclinical studies: solid orthotopic and heterotopic grafts of human gliomas into nude mice. J. Neurosci. Methods *125*, 147–157.

Tsuzuki, Y., Fukumura, D., Oosthuyse, B., Koike, C., Carmeliet, P., and Jain, R.K. (2000). Vascular endothelial growth factor (VEGF) modulation by targeting hypoxia-inducible factor-1$\alpha \to$ hypoxia response element$\to$ VEGF cascade differentially regulates vascular response and growth rate in tumors. Cancer Res. *60*, 6248–6252.

Unruh, A., Ressel, A., Mohamed, H.G., Johnson, R.S., Nadrowitz, R., Richter, E., Katschinski, D.M., and Wenger, R.H. (2003). The hypoxia-inducible factor-1α is a negative factor for tumor therapy. Oncogene *22*, 3213–3220.

Watnick, R.S., Cheng, Y.N., Rangarajan, A., Ince, T.A., and Weinberg, R.A. (2003). Ras modulates Myc activity to repress thrombospondin-1 expression and increase tumor angiogenesis. Cancer Cell *3*, 219–231.

Xiao, A., Wu, H., Pandolfi, P.P., Louis, D.N., and Van Dyke, T. (2002). Astrocyte inactivation of the pRb pathway predisposes mice to malignant astrocytoma development that is accelerated by PTEN mutation. Cancer Cell *1*, 157–168.

Yancopoulos, G.D., Davis, S., Gale, N.W., Rudge, J.S., Wiegand, S.J., and Holash, J. (2000). Vascular-specific growth factors and blood vessel formation. Nature *407*, 242–248.

Zagzag, D., Zhong, H., Scalzitti, J.M., Laughner, E., Simons, J.W., and Semenza, G.L. (2000). Expression of hypoxia-inducible factor 1α in brain tumors: association with angiogenesis, invasion, and progression. Cancer *88*, 2606–2618.